

963

# NATIONAL ADVISORY COMMITTEE FOR AERONAUTICS

CASE FILE  
COPY

TECHNICAL NOTE

No. 963

FRICITION IN PIPES AT SUPERSONIC AND SUBSONIC VELOCITIES

By Joseph H. Keenan and Ernest P. Neumann  
Massachusetts Institute of Technology

PROPERTY FAIRCHILD  
ENGINEERING LIBRARY



Washington  
January 1945

NATIONAL ADVISORY COMMITTEE FOR AERONAUTICS

-----  
TECHNICAL NOTE NO. 963  
-----

FRICITION IN PIPES AT SUPERSONIC AND SUBSONIC VELOCITIES

By Joseph H. Keenan and Ernest P. Neumann

SUMMARY

The apparent friction coefficient was determined experimentally for the flow of air through smooth pipes at subsonic and supersonic velocities. Values of the Mach number ranged from 0.27 to 3.87 and of Reynolds number from  $1 \times 10^5$  to  $8.7 \times 10^5$ . In supersonic flow the results were found to be strongly influenced by the presence of oblique shocks formed at the junction of nozzle and pipe. The effect of these shocks on the coefficient of friction was determined. Nozzle forms were devised which eliminated the shocks and their effects.

It was found that at distances from the pipe inlet greater than 50 diameters the apparent coefficient of friction for compressible flow at Mach numbers greater or less than 1 is approximately equal, for equal Reynolds numbers, to the coefficient of friction for incompressible flow with completely developed boundary layer. Mach numbers greater than 1 are rarely maintained for lengths of 50 diameters. For attainable lengths the coefficient of friction is a function of the ratio of length to diameter and the Reynolds number, with the Mach number at entrance determining the maximum attainable length.

INTRODUCTION

The effect of friction on the flow of compressible fluids in pipes of uniform cross-sectional area was investigated analytically by Grashof (reference 1) and Zeuner (reference 2) who arrived at a relationship between velocity and friction coefficient for perfect gases. Stodola (reference 3) showed that the curves of Fanno permit a general

graphical treatment for any law of friction. Frössel (reference 4) presented the first extensive measurements of friction coefficients for the flow of air through a smooth tube with velocities above and below the velocity of sound. His measured coefficients for both subsonic and supersonic compressible flow appear to be in excellent agreement at corresponding Reynolds numbers with coefficients measured for incompressible flow. Keenan (reference 5) presented experimental data on commercial pipe for the flow of water and for the flow of steam at subsonic velocities. These indicated that the friction coefficient is the same for the same Reynolds number for an incompressible fluid and for subsonic flow of a compressible fluid.

In the subsonic region the measurements of Frössel and of Keenan were in accord in that they revealed no variation of the friction coefficient that was peculiar to compressible fluids. In the supersonic region the measurements of Frössel pointed to a similar conclusion. Frössel's data for this region were published as a chart (fig. 7 of reference 4) which, despite its small scale, seemed to reveal great irregularities in the data. The friction coefficients, which were computed from the derivatives of the curves through the experimental points, must have been subject to great uncertainty.

This investigation, conducted at Massachusetts Institute of Technology, was sponsored by and conducted with the financial assistance of the National Advisory Committee for Aeronautics.

#### SYMBOLS

- a cross-sectional area of test pipe (sq ft)
- D diameter of test section (ft)
- d throat diameter of nozzle
- F wall-friction force (lb)
- G mass rate of flow per unit area (lb/sq ft sec)
- g acceleration given to unit mass by unit force (ft/sec<sup>2</sup>)
- h enthalpy (ft-lb/lb)

- k ratio of specific heats
- L length of test section (ft)
- M Mach number
- P pressure (lb/sq ft abs.)
- Re Reynolds number
- T temperature (F abs.)
- $T_m$  mean stream temperature at a given cross section of the test pipe (F abs.)
- $T_i$  mean stream temperature at the initial state of the fluid stream, that is, where  $V = 0$  (F abs.)
- V mean velocity of the fluid stream at a given cross section of the test pipe (ft/sec)
- v specific volume (cu ft/lb)
- w mass rate of flow (lb/sec)
- x distance along test section (ft)
- $\lambda$  friction coefficient  $\frac{\tau}{\frac{1}{2} \rho V^2}$
- $\lambda_c$  friction coefficient calculated from
- $$\frac{1}{\sqrt{4\lambda_c}} = -0.8 + 2 \log Re \sqrt{4\lambda_c}$$
- with Re based on  $T_m$
- $\lambda_i$  friction coefficient calculated from above-mentioned equation with Re based on  $T_i$
- $\rho$  mass density  $\left(\frac{1}{vg}\right)$
- $\tau$  friction force per unit of wall surface (lb/sq ft)
- $\theta$  angle between walls of entrance nozzle

## Subscripts

- $i$  refers to the initial state of the fluid stream where the velocity is zero
- $1$  and  $2$  refer to arbitrary datum sections along the test pipe

## Constants used in calculations

- $k$  ratio of specific heats (1.400)
- $c_p$  specific heat at constant pressure (0.240 Btu/F lb)
- $A$  number of foot-pounds in 1 Btu (778.3)

## OBJECT

Some preliminary investigations (reference 6) into supersonic flow of air which were made in the Laboratory of Mechanical Engineering at the Massachusetts Institute of Technology indicated friction coefficients appreciably different from those reported by Frössel. The present investigation was undertaken in an attempt to resolve this disagreement and to obtain some dependable experimental data on supersonic flow with friction. In order to tie the investigation into previous studies of the flow of incompressible fluids some measurements of subsonic flow were included.

## TEST APPARATUS

The arrangement of the test apparatus is shown in figure 1. Air is supplied by either a two-stage, steam-driven compressor or a rotary, electric-driven compressor. At the discharge from the compressor is a receiver to smooth out fluctuations in flow. For some tests a dehumidifying system was used to remove moisture from the air leaving the compressor. This dehumidifying system consists of a cooling coil followed by a heating coil. It is connected into the system as shown in figure 1.

The air stream is introduced into the test pipe through a rounded-entrance nozzle of circular cross section. Details of the nozzles used in different tests are shown in figures 2 to 5.

The test pipe is in each instance a piece of standard drawn brass tubing. For the subsonic tests the inside diameter of the tube was 0.375 inch. For the supersonic tests three tubes were used having inside diameters of 0.4375, 0.498, and 0.945 inch, respectively.

The air stream leaving the test pipe is discharged either to the atmosphere or to an ejector which uses steam as the primary fluid.

The pressure measurements, from which the friction coefficients are calculated, were made at holes of 0.020-inch diameter drilled in the tube wall. To avoid a burr at the inside edges of the pressure holes, the inside of the test pipe was carefully polished with fine emery cloth. Connections between the pressure holes, manifolds, and manometers are made with 1/4-inch copper tubing.

All pressure differences were measured with simple U-tube manometers. In the supersonic test the pressures in the test pipe were generally small fractions of an atmosphere. They were measured with an absolute mercury manometer. With the aid of a sliding marker on the manometer scales, pressure differences could be read to 0.01 centimeter. Pressures higher than 50 psi gage before the inlet nozzle were measured with a calibrated Bourdon gage; lower pressures were measured with a mercury column.

The temperature of the air stream in front of the nozzle could be measured by either a copper-constantan thermocouple or a mercury-in-glass thermometer. Readings usually were made with the thermometer.

The discharge coefficient for the 0.375-inch diameter subsonic nozzle was determined by means of a gasometer. The discharge coefficients for each supersonic nozzle were obtained from the A.S.M.E. data on nozzle coefficients (reference 7).

## METHOD OF TESTING

The air compressor was started and sufficient time allowed to elapse to obtain steady-state conditions before any readings were taken. Temperature readings were taken at definite intervals of time. Pressure differences between a given pair of taps were measured on either a mercury manometer or a water manometer depending upon the magnitude of the difference to be measured. In order to establish a continual check against possible leakage from either of the two manifolds, pressure differences were recorded for each pair of taps, with the higher pressure first in one manifold and then in the other. To check against possible leakage from the connections between the pressure taps and the manifold, a soap-and-water solution was applied at each connection. For the supersonic runs, where the pressures measured were below atmospheric pressure, the manometer system was tested by subjecting it to a pressure higher than atmospheric before starting a test.

## RESULTS OF TESTS

## The Apparent Friction Coefficient

The results of these tests are shown principally in terms of the apparent friction coefficient  $\lambda$ . This term is intended to represent for any cross section of the stream the quantity

$$\frac{2\tau}{\rho V^2}$$

where  $\tau$  denotes the shear stress at the pipe wall,  $\rho$  the mean density, and  $V$  the mean velocity. In reality the apparent friction coefficient is defined in terms of the measured quantities, flow per unit area, and pressure, through equation (8), together with equation (7), of appendix A. Equation (8) is identical with the statement

$$\lambda = \frac{2\tau}{\rho V^2}$$

if the velocity across each section is so nearly uniform that the mean velocity found from the flux of kinetic energy

is identical with that found from the flux of momentum, or if the flux of momentum and the flux of kinetic energy do not change from section to section.

The flow of an incompressible fluid in a pipe at a great distance downstream from the entrance satisfies the latter condition. The flow of a compressible fluid satisfies neither condition. It is probable, however, that the former is nearly satisfied in compressible flow at a great distance downstream from the entrance, provided the longitudinal pressure gradient is not inordinately large.

The magnitude of the true friction coefficient ( $2\tau/\rho V^2$ ) can be found only from a determination of the magnitude of the shear stress at the pipe wall. If the shear stress is to be measured directly, the experimental difficulties are formidable; if it is to be deduced from pressure measurements, either the analytical difficulties or the uncertainties introduced by supposition are likely to prove discouraging.

The apparent friction coefficient, on the other hand, may be rather simply deduced from common types of measurement. Moreover, when its value is known it may be readily applied to the design of passages.

The adoption of the apparent friction coefficient for reporting the results of measurements of the type presented here will facilitate comparison between data from different sources. The calculation of the apparent friction coefficient involves the simplest calculation and the minimum extraneous hypothesis consistent with reducing the measurements to a basis of comparison. The tests of Frössel (reference 4) and Keenan (reference 5) have been so presented.

In all subsequent paragraphs the term friction coefficient is to be interpreted to mean apparent friction coefficient as defined by equation (8).

### Subsonic Flow

The results for the subsonic tests are presented in tables I to IV. The variation in pressure along the length of the test pipe is shown in figure 6. For test 1 the pressure in the exhaust space after the end of the pipe was below the sound pressure - that is, the pressure at the state of maximum entropy; consequently, the flow through the pipe



was the maximum flow corresponding to the initial condition of the air stream. For test 2 the air stream was throttled behind the pipe and for tests 3 and 4 in front of the pipe, to produce pressures at the pipe exit in excess of the sound pressure, which resulted, in turn, in a flow less than the maximum flow for the existing initial conditions.

The friction coefficients corresponding to the intervals of pipe length between pressure taps are given in tables I to IV. In figure 7 the arithmetic mean of these values of the friction coefficient for each test is plotted against the arithmetic mean of the Reynolds number for that test. The length interval from 0 to 1 foot was omitted from the calculation of the mean because the velocity profile was doubtless changing greatly in this interval. The last 3 inches of length also were omitted because of the effect on velocity and pressure distribution of the abrupt discharge into the exhaust space. Thus the data of figure 7 correspond to a well-developed boundary layer and as stable a velocity profile as the conditions of compressible flow permit.

The Von Kármán-Nikuradse relation between friction coefficient and Reynolds number for incompressible flow is shown by the curve on figure 7. The greatest discrepancy between the present results and this curve is of the order of 3 percent, which is approximately the degree of uncertainty in the present measurements.

Figures 8 and 9 show the variation along the length of the tube of friction coefficient, mean temperature, and Mach number for tests 1 and 2. The values of friction coefficient for incompressible flow corresponding to the Reynolds number at each point along the length of the pipe are shown by the dash curve of figure 8. In test 1 the Mach number ranges from 0.32 to 1 and in test 2 from 0.3 to 0.47. In both tests, however, the agreement between the measured friction coefficients and those for incompressible flow is consistently good. This agreement confirms the conclusion reached by Keenan and by Frössel that for subsonic velocities the friction coefficient is a function of the Reynolds number and is not appreciably affected by change in the Mach number.

#### Supersonic Flow

Length of test pipe.- The length of the test pipe for supersonic tests is limited by the divergence ratio of the

nozzle that feeds the pipe. For a given divergence ratio and a given nozzle efficiency, a maximum length of test pipe exists for which a transverse pressure shock will not appear in a pipe. For greater lengths a shock appears, and this shock moves closer to the nozzle as the length is increased. Since the velocity of the stream on the downstream side of the shock is always subsonic, the maximum length of supersonic flow is attained in the longest pipe without a pressure shock. Considerations which govern the length of subsonic and supersonic flow are presented in appendix B. The maximum length of supersonic flow attained in the present tests is 50 diameters.

The Nozzle. - If the junction between the divergent nozzle passage and the test pipe is not properly designed, an oblique shock wave will form at or near the junction. This wave will extend down and across the stream until it encounters the opposite wall and then will reflect back and forth along the length of the pipe. Figure 10, from the thesis of Huron and Nelson (reference 8), shows such oblique waves in a two-dimensional nozzle. Since in crossing the oblique shock the pressure rise in the stream is almost discontinuous, measurements of pressure variation along the test pipe become difficult to interpret. Moreover, it appears probable that the existence of the shock stimulates thickening of the boundary layer and so influences strongly the magnitude of the friction coefficient. Under extreme conditions the oblique shock may initiate separation of the stream from the wall.

With the aid of the method of Shapiro (reference 9) nozzles were designed so as to introduce the stream into the test pipe without the formation of an oblique shock of sufficient intensity to affect the measured pressures. Figure 11 (from reference 8) shows the flow from a two-dimensional nozzle which is comparable to the test nozzles and which was designed by the same method. The first photographs, taken by the schlieren method, of flow through this nozzle showed a clear field in both nozzle and tube. In order to make visible the pattern of flow and to demonstrate that shock waves if present would be discernible, the walls of the nozzle and the parallel passage were knurled. Each rib of the knurling set up a disturbance of small magnitude which extended across the stream in the manner of an oblique shock. Since the presence of these small disturbances could be detected, the presence of an oblique shock would also be detected. The walls at the junction of the nozzle and tube and for a short interval in the passage a little distance

downstream from the junction were left unknurled to permit a shock to be more readily distinguished, but none appeared.

The effect of angle of divergence.- To determine the effect on the apparent friction coefficient of oblique shocks in the test pipe, a series of tests were made using entrance nozzles with conical divergent sections of different angles of divergence  $\theta$ . The junction of the nozzle and pipe was in each case a sharp corner.

The variation in pressure along the test pipe for various values of the angle of divergence is shown in figure 12. For an angle of  $24^\circ$  the pressure decreases along the first 10 diameters of pipe length. This decrease appears to be an extension of the expansion from the nozzle into the test pipe. It is doubtless caused by separation of the stream from the walls of the nozzle.

For angles of  $12^\circ$  or less the rise in pressure across the corner at the junction was measured by means of pressure taps located immediately before and after the corner. The measured pressure rise is shown in each instance by the interval between the two points at zero value of  $L/D$ . The ratio of pressures across the joint varies from 1.30 for an angle of  $12^\circ$  to 1.03 for an angle of  $2^\circ$ . The departure from 1 in the latter figure is hardly in excess of the uncertainty in the pressure measurements. For an angle of  $6^\circ$  the ratio is 1.16. The analysis of Meyer (reference 10) indicates a pressure ratio of 1.22 across the oblique shock arising from a change of direction of  $3^\circ$  at a Mach number of 2.29. This analysis is applicable only to two-dimensional flow which the flow near the tube wall should approximate. The experimental and analytical values appear to be of the same order of magnitude.

It may be seen from figure 12 that as the angle of divergence decreases the pressure rise at the junction decreases and the curve of pressure against distance becomes smoother. With a nozzle designed for shock-free conditions the curve becomes smooth and the rise in pressure at the junction becomes zero within the precision of the pressure measurements.

Although measurements made under other than shock-free conditions are not considered valid, a study was made of the effect on the apparent friction factor of nozzles of the ordinary type. Such nozzles were used, presumably, by

Frössel who gave no indication that he had developed a special nozzle for the purposes of his tests. The friction coefficients computed from the curves of figure 12 are plotted in figure 13 against the angle of divergence of the nozzle. These friction coefficients are the mean coefficients for the interval of length between values of  $L/D$  of 1.59 and 27.0. This interval was chosen because it was approximately the same as that used by Frössel.

According to the data of figure 13 the friction coefficient for a given Reynolds number approaches the Von Kármán-Nikuradse value for incompressible flow as the angle of divergence increases. Perhaps this is evidence of the increase in thickness of the boundary layer caused by the oblique shock. The Von Kármán-Nikuradse value is obtained from flow at large values of  $L/D$ , where the boundary layer fills the cross section and turbulence is fully developed. In supersonic flow the presence of an oblique shock may have an effect on the boundary layer similar to the effect of length in incompressible flow.

The apparent friction coefficient.- The apparent friction coefficient  $\lambda$  is plotted against distance from the entrance to the test pipe in figure 14. Data for the tests shown in figure 14 are presented in tables V to IX. The two extremities of the horizontal line which passes through each test point of figure 14 show, respectively, the positions at which the two pressures used in calculating the value of the friction coefficient were measured. Thus each point represents a mean value of the apparent friction coefficient over a short interval of length. The pressure difference across this interval was in each instance very small, and any irregularity in the pressure distribution or any error in a pressure measurement had, therefore, an exaggerated effect on the calculated friction coefficient. For this reason the points of figure 14 scatter over a band of considerable width. Nevertheless a definite pattern is discernible which is common to all five sets of data. Near the entrance to the test pipe the coefficient decreases sharply with increasing distance along the pipe. At a distance of 5 to 10 diameters the coefficient passes through a minimum. At greater distances there is evidence of a maximum followed by another minimum.

The data of figure 14 are not sufficiently precise to establish the number of maxima and minima or the amplitude of the fluctuations in the value of the coefficient, but an

attempt to approximate these is represented by the solid lines of figure 14. A somewhat similar variation in friction coefficient near the entrance to a pipe has been shown for flow of an incompressible fluid by Kirsten (reference 11) and by Brooks, Craft, and Montrello (reference 12). It is doubtless a phenomenon relating to the transition from laminar to turbulent flow in the boundary layer. No exact correspondence between pairs of curves of figure 14 should be expected because the degree of development of the boundary layer at pipe entrance varied from test to test with the length and other dimensions of the nozzle. The one exception is the pair of curves in the middle of the figure which were obtained with the same nozzle and test pipe.

On each of the charts of figure 14 are shown by dash lines values of the friction coefficients  $\lambda_i$  and  $\lambda_c$  calculated from the Von Kármán-Nikuradse relation for incompressible fluids. The coefficients  $\lambda_i$  and  $\lambda_c$  are calculated using, respectively, the Reynolds numbers corresponding to the viscosity at the temperature before the inlet nozzle where the velocity is zero and that at the mean stream temperature. In view of the "recovery" of temperature in the boundary layer some value intermediate between these two would seem to be most appropriate.

For distances from the entrance greater than 20 diameters the trend of the coefficient is definitely upward. The limit of this trend appears to be a horizontal line or a curve with ordinates approximately equal to  $\lambda_i$  or  $\lambda_c$ .

The five charts of figure 14 may be roughly grouped into those of high Reynolds number, the left-hand three, and those of low Reynolds number, the right-hand two. The left-hand group of curves shows a distinct similarity in pattern and position; whereas the right-hand group shows in comparison lower values at the minimum point and higher values at large values of  $L/D$ .

No analogous trend with Mach number can be discerned. Although the top and middle charts in the left-hand group have Mach numbers at entrance of 2.06 and 3.09, respectively, they differ less than the two middle charts which have Mach numbers of 3.09 and 2.84, respectively. Differences appear to depend upon Reynolds number rather than Mach number.

To test whether the changes in characteristics were the result merely of accidental differences between test pipes and entrance nozzles, two tests were run with the same test pipe and nozzle at approximately the same Mach number but with different Reynolds numbers. These are shown by the two middle charts of figure 14. The differences between these two charts are consistent with the differences between any other pair of charts for two different Reynolds numbers.

The conclusion seems tenable, therefore, that for values of  $L/D$  greater than 50 the apparent coefficient of friction for compressible flow at Mach numbers greater or less than 1 is approximately equal, for equal Reynolds numbers, to the coefficient of friction for incompressible flow.

For Mach numbers greater than 1, however, values of  $L/D$  greater than 50 are rarely encountered; and for values less than 50 the apparent coefficient of friction is generally less than that given by the Von Kármán-Nikuradse formula for the same Reynolds number. Since the present tests do not exceed a Reynolds number of  $8.7 \times 10^5$ , this last conclusion is open to question if the Reynolds number exceeds 1,000,000.

Because of a slight irregularity at the junction of the nozzle and the test pipe, the data of test 12 at small values of  $x/D$  were considered to be less reliable than those of the other tests. The data of test 12 are, nevertheless, in substantial accord with those of the other tests. If they were shown in figure 15, they would not alter in any way the conclusions drawn below. The figure is somewhat simplified by omitting them.

The mean apparent friction coefficient.- In figure 15 the mean apparent friction coefficient between the entrance to the test pipe and any value of  $L/D$  is plotted against that value of  $L/D$ . This method of plotting has two advantages - first, this mean friction coefficient is more readily applied to design calculations than the more nearly point values of figure 14; second, since it is computed, in general, from a larger measured pressure difference, the values of the ordinate of figure 15 are less affected by small experimental errors and irregularities and, therefore, yield a smoother curve.

The curves of figure 15, consistently with those of figure 14, show certain trends with increasing Reynolds number: the point of minimum mean friction coefficient moves to

lower values of  $L/D$ , and the rate of increase of friction coefficient with  $L/D$  at the higher values of  $L/D$  decreases. On each curve is given the Reynolds number corresponding to the viscosity at zero velocity (the "complete-recovery" value), and at the right-hand margin is shown the corresponding value of the coefficient of friction for an incompressible fluid at large values of  $L/D$ .

The experimental curves are extrapolated in figure 15 as they would go if the values for incompressible flow were the asymptotes. The extrapolations cannot, however, extend to the asymptotes. It is explained in appendix B that for a fixed value of the Mach number at entrance there is a corresponding maximum value of  $\lambda L/D$ , as shown in figure 16. That maximum value represents an equilateral hyperbola cutting across figure 15. Segments of such hyperbolas are shown for entrance Mach numbers of 1.5, 2, 3, 4, and infinity. For an entrance Mach number of 1 the corresponding hyperbola is formed by the two axes of coordinates, and the maximum value of  $L/D$  is zero for any finite value of  $\lambda$ .

At the lower values of  $L/D$  some variation from the curves of figure 15 may be expected if the nozzle design is not identical with the corresponding one employed here. Large departures from these values will result, as indicated in figure 13, if oblique shocks are formed at the junction of nozzle and test pipe. But with a carefully designed nozzle and a smooth test pipe the mean apparent friction coefficient should be in close accord with the curves of figure 15.

#### COMPARISONS

In subsonic flow two previous experimental investigations by Keenan (reference 5) and Frössel (reference 4) indicated that for large values of  $L/D$  the apparent friction coefficient is essentially independent of Mach number and is, within experimental error, the same function of Reynolds number as the friction coefficient for incompressible fluids. The present investigation, as shown by figure 7, confirms these conclusions.

In supersonic flow the only previous experimental investigation is that of Frössel (reference 4). His conclusion is the same as for subsonic flow - namely, that the

apparent friction coefficient at the attainable values of  $L/D$  is the same function of Reynolds number as the friction coefficient for incompressible fluids at large values of  $L/D$ . The present investigation does not confirm this conclusion. It indicates that the apparent friction coefficient is a function of  $L/D$  as well as Reynolds number over the attainable range of  $L/D$ , and that the effect of Mach number is to limit the range of values of  $L/D$ .

Frössel concludes that his measured friction coefficients are represented within the precision of measurement by the Von Kármán-Nikuradse relation. Thus, the comparisons of this relation with the present data, as given in figures 14 and 15, are in effect comparisons of Frössel's data with the present data. It should be remembered, however, that Frössel's data for supersonic velocities spread over a band with a width of about 20 percent, and that the method of computing them seems to leave much room for uncertainty.

Frössel offers no discussion of the development of nozzles suitable to his purpose, and the only published illustrations of his nozzles are to such a small scale that little dependable information can be obtained from them. These illustrations, however, are not inconsistent with the assumption that his nozzles were of the conical type with an angle of divergence in the order of  $15^\circ$ . The data of figure 13 indicate that for angles of this magnitude Frössel's conclusions have been confirmed. For supersonic flow without oblique shocks, however, the conclusions of Frössel have not been confirmed.

The classical analysis of flow with friction through a pipe of constant cross-sectional area is based on the assumption that the velocity is uniform over any cross section. Hawthorne (reference 13) used this analysis to show that the product of the maximum  $L/D$  and the mean apparent friction coefficient over the length  $L$  is a unique function of the Mach number at entrance. The form of this function is shown by curves A and C in figure 16, and the abscissas of curve A determine the position of the curves of maximum  $L/D$  for Mach numbers of 1.5, 2, 3, 4, and infinity in figure 15.

From this same analysis may be calculated the minimum exit pressure for subsonic flow and the maximum exit pressure for supersonic flow. The ratios of these pressures to the pressure at pipe inlet may be found from figure 16 from the intersections of the curves of constant  $p_2/p_1$  with curves A and C.



For subsonic conditions the minimum exit pressure for a given length of pipe is obtained by lowering the pressure in the exhaust space until the pressure in the exit plane ceases to fall. Then the entrance Mach number corresponding to the exit-plane pressure may be determined by measurements at the inlet. In figure 6 the measured pressure from the tap nearest the exit plane is compared with the calculated minimum pressure (the pressure of maximum entropy). The measured pressure falls slightly below the calculated minimum. This is in accord with similar observations made by Frössel.

In supersonic flow an experimental determination of the maximum pressure is more difficult. The divergence ratio of the nozzle fixes the Mach number at entrance. The maximum pressure will be attained at the exit only if the pipe attached to the nozzle is the longest pipe which will not cause a transverse pressure shock. The maximum pressure cannot be attained, therefore, although it may be approximated closely by a tedious method of trial and error. Where it has been nearly attained in these tests, it has always been slightly less than the calculated maximum.

In a revision of the classical analysis Young and Winterbottom (reference 14) took "account of the development of the boundary layer, the variation of density across any section of the pipe, and the variation in the frictional coefficient along the pipe." The boundary layer was assumed to be completely turbulent. They show graphically to a small scale the calculated variation in pressure and true friction coefficient,  $2\tau/\rho_0 V_0^2$ , in terms of the density  $\rho_0$  and the velocity  $V_0$  at the inlet cross section of the pipe. For the larger values of  $L/D$  these values appear to be in accord with figure 15. For the smaller values of  $L/D$  the small scale of the diagrams precludes any comparison.

These authors present comparisons of their results with the experiments of Frössel and the calculations of Hawthorne. It appears, however, that they have compared mean values of their own true friction coefficients with the apparent friction coefficients of Frössel and Hawthorne, and the comparisons are therefore invalid.

## CONCLUSIONS

For values of  $L/D$  greater than 50 the apparent coefficient of friction for compressible flow at Mach numbers greater or less than 1 is approximately equal, for equal Reynolds numbers, to the coefficient of friction for incompressible flow with completely developed boundary layer.

For Mach numbers greater than 1, however, values of  $L/D$  greater than 50 are rarely encountered. For values of  $L/D$  less than 50 the coefficient of friction is a function of  $L/D$  and Reynolds number. It is generally less than that given by the Von Kármán-Nikuradse formula if the Reynolds number is less than  $10^6$ . The effect of Mach number is to limit the range of values of  $L/D$ .

For Mach numbers greater than 1 the mean apparent coefficient of friction decreases rapidly from a relatively high value at entrance to a minimum value which it attains within a distance of 20 diameters from the entrance. Beyond this minimum point the mean coefficient rises with increasing distance along the tube and appears to approach as a limit the value given by the Von Kármán-Nikuradse formula. The point values of the apparent coefficient appear to attain the formula value at a distance of approximately 50 diameters from the tube entrance - the mean values of the coefficient would attain the limit at perhaps twice this distance from the entrance.

The variation in coefficient of friction with  $L/D$  for supersonic flow is similar to that observed in the flow of incompressible fluids. An adequate comparison cannot be made, however, until more extensive information is available as to the effect of  $L/D$  in the flow of incompressible fluids.

The minimum observed pressure in subsonic pipe flow and the maximum observed pressure in supersonic pipe flow are each slightly less than the value calculated on the basis of the assumption that the velocity is uniform across any section.

The apparent coefficient of friction is strongly influenced by the presence of oblique shock waves in the tube.

The junction of the tube with an ordinary conical nozzle causes oblique shock waves, the amplitude of which increases with increasing angle of the cone. The apparent coefficient of friction also increases with increasing angle of the nozzle cone, and appears to attain approximately the Von Kármán-Nikuradse value when the angle of the cone is  $15^\circ$  or more.

Department of Mechanical Engineering,  
Massachusetts Institute of Technology,  
Cambridge, Mass., April 1944.

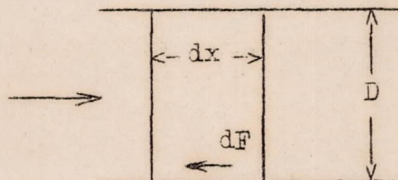
## APPENDIX A

### METHOD OF ANALYSIS

The analysis that follows, except for certain minor changes to follow the notation of this paper, has been taken verbatim from the appendix of reference 5.

#### Dynamic Equation for Flow in Pipe of Constant Cross-Sectional Area

Consider an element of fluid which is bounded by two parallel planes transverse to the direction of flow and a distance  $dx$  apart. The forces acting on this element may



be classified as normal forces corresponding to hydrostatic pressures and shearing forces corresponding to wall friction.

It can be shown that Newton's Second Law becomes for steady flow

$$-a dp - dF = (w/g) DV \quad (1)$$

where  $a$  denotes the cross-sectional area of the passage,  $dp$  the increase in hydrostatic pressure of the fluid across distance  $dx$ ,  $dF$  the wall-friction force applied to the stream between the two planes,  $w$  the mass rate of flow,  $g$  the acceleration given to unit mass by unit force, and  $DV$  the increase in the mean velocity of the stream across  $dx$ .

The wall-friction force  $dF$  may be expressed in terms of a friction coefficient which is commonly defined by the relation

$$\lambda = \frac{\tau}{\frac{1}{2} \rho V^2}$$

where  $\lambda$  denotes the friction coefficient,  $\tau$  the friction force per unit of wall surface, and  $\rho$  a mass density of the fluid which is otherwise  $1/vg$ . Then we may write

$$dF = \tau \pi D dx = \lambda V^2 \pi D dx / 2vg$$

where  $D$  is the pipe diameter and  $dx$  is an element of length along the pipe. Substituting this expression for  $dF$  in equation (1) dividing through by  $av$  and rearranging, we get

$$\frac{dp}{v} + \frac{G}{gv} dV + \frac{\lambda}{2} \left(\frac{V}{v}\right)^2 \frac{\pi D}{ag} dx = 0$$

where  $G$  is  $w/a$ . Since  $G$  for steady flow is constant along the length of the pipe and equal to  $V/v$ , the last equation may be written in the form

$$\frac{dp}{v} + \frac{G^2}{g} \frac{dv}{v} + \frac{2\lambda G^2}{Dg} dx = 0 \quad (2)$$

This is the dynamic equation of flow through a pipe. It may be used to determine the mean friction coefficient between two cross sections as follows:

Assume  $\lambda$  to be constant between sections 1 and 2. Then equation (2) integrates to the expression

$$\int_1^2 \frac{dp}{v} + \frac{G^2}{g} \ln \frac{v_2}{v_1} + \frac{2\lambda G^2}{Dg} (x_2 - x_1) = 0 \quad (3)$$

which may be solved for  $\lambda$ . In an actual case  $\lambda$  may be interpreted as the mean coefficient of friction. For a numerical solution it is necessary to know not only the dimensions of the pipe and the rate of fluid flow, but also the relationship between pressure and specific volume along the path of flow.

#### The Pressure-Volume Relationship

Let us consider the adiabatic case, that is, the case in which heat flow to or from the fluid stream is negligible. Then from the first law of thermodynamics we know that for any section  $a$  along the pipe length the sum of the enthalpy and kinetic energy per unit mass of fluid crossing that section is constant and is equal to the enthalpy at a preceding section  $i$ , where the cross-sectional area is very large and the kinetic energy is negligible: Thus

$$h + V^2/2g = h_i \quad (4)$$

where  $h_i$  denotes the enthalpy at section  $i$  and the symbols without subscript denote quantities corresponding to section  $a$ . Substituting  $Gv$  for  $V$  in equation (4) we get

$$h + \frac{G^2 v^2}{2g} = h_i \quad (5)$$

Equation (5) yields a series of relationships between  $h$  and  $v$ .

Having determined by measurements the initial state  $i$  and the mass rate of flow per unit area  $G$  of a stream flowing through the pipe, we may determine by equation (5) the  $h$ - $v$  relationship.

For a perfect gas

$$h = \frac{k}{k-1} pv = Bpv \quad (6)$$

where  $k$  is the ratio of the specific heats and  $B$  is a constant defined by equation (6).

Substituting equation (6) into the Fanno-line equation (5) we get

$$h_i = \frac{G^2 v^2}{2g} + Bpv \quad (7)$$

which, for given values of  $h_i$  and  $G$ , is a pure pressure-volume relation. Solving equation (7) for  $p$ , differentiating, and dividing through by  $v$  we get for the first term of equation (2)

$$\frac{dp}{v} = - \frac{G^2}{2gB} \frac{dv}{v} - \frac{h_i}{B} \frac{dv}{v^3}$$

#### Friction Coefficient

Substituting the last expression into equation (3) and integrating between sections 1 and 2, we get

$$\frac{G^2}{g} \left(1 - \frac{1}{2B}\right) \ln \frac{v_2}{v_1} + \frac{h_i}{2B} \left(\frac{1}{v_2^2} - \frac{1}{v_1^2}\right) + \frac{2G^2 \lambda (x_2 - x_1)}{gD} = 0$$

or

$$\lambda = \frac{gD}{2G^2 (x_2 - x_1)} \left[ \frac{c_p T_1 A (k-1)}{2k} \left(\frac{1}{v_1^2} - \frac{1}{v_2^2}\right) - \frac{G^2 (k+1)}{g} \ln \frac{v_2}{v_1} \right] \quad (8)$$

If measurements are made of the initial state, the rate of flow, and the pressures at 1 and 2, the values of  $v_1$  and  $v_2$  can be found by solving the quadratic equation (7). The friction coefficient may then be computed from equation (8).

This analysis is oversimplified in that a single velocity  $V$  is associated with a given cross section of the stream and this velocity is assumed to be identical with the mean velocity of flow  $Gv$ , where  $v$  denotes the mean specific volume. It is probable that the friction coefficient

so derived may be used to calculate wall friction whenever the section is sufficiently far from the entrance to the tube that variation in that distance will not appreciably alter the pattern of flow if velocity, pressure, and other factors remain unchanged. In subsonic flow such conditions are doubtless attained except in very short tubes; however, in supersonic flow these conditions may not be attained at all because of the rapid change in pressure and velocity along the tubes of even the greatest possible lengths. The friction coefficient so calculated may be called the apparent friction coefficient.

In the present state of knowledge of supersonic flow it is uncertain how closely the product of  $\lambda$  and  $\frac{1}{2}\rho V^2$  approximates the shear stress  $\tau$  at the wall of the pipe. It appears probable, however, that, with some exceptions, the apparent friction coefficient will prove adequate for design of passages in supersonic flow. The apparent friction coefficient is at least the analogue of the friction coefficient for incompressible flow and as such its variation with the usual parameters is of interest. The apparent friction coefficient also permits a direct comparison of the variation of static pressure along the path of flow for various tests. Frössel's tests were reported in terms of this apparent friction coefficient.

The value of the viscosity employed in calculating the Reynolds number  $Re$  and that of the velocity of sound in the Mach number  $M$  correspond to the mean state of the fluid at any cross section. This mean state is determined from the measured pressure and the specific volume as found by solving equation (7). The viscosity was in turn found from Sutherland's formula - namely, viscosity (in centipoises)

$$= 0.01709 \frac{491.6 + 205.2}{T + 205.2} \left( \frac{T}{491.6} \right)^{3/2} .$$

## APPENDIX B

### ANALYTICAL RELATIONS

#### Possible Ranges of Subsonic and Supersonic Flow

The relation between length of flow, pressure change, and mean friction coefficient for a stable velocity

distribution is shown in figure 16. The curves shown were computed from the relations derived in appendix A.

The region in figure 16 lying below curve C represents conditions of subsonic flow throughout the tube. The region lying above curve A represents conditions of supersonic flow throughout the tube.

Within each of these regions are shown lines of constant ratio of the pressure at the exit of an interval of tube length to the pressure at the entrance. If the Mach number at entrance, the tube diameter, and the tube length between two measured pressures are known, the friction coefficient  $\lambda$  may be found from figure 16. Conversely, for a given value of  $\lambda$  the pressure distribution along the length of a tube may be found for any value of the Mach number at the entrance. The curves of constant pressure ratio in the supersonic region are valid only if no shock occurs in the length of tube to which they are applied.

Curve A shows the maximum value of  $\lambda \frac{L}{D}$  for supersonic flow for each value of the Mach number at the entrance, and curve C shows the corresponding value of  $\lambda \frac{L}{D}$  for subsonic flow. Along each of these curves the Mach number at the tube exit is 1. In the tube corresponding to curve A the Mach number decreases in the direction of flow; whereas in the tube corresponding to curve C the Mach number increases.

Curve A indicates that the value of  $\lambda \frac{L}{D}$  for supersonic flow in a tube may be increased by increasing the Mach number at entrance, which is accomplished by increasing the divergence ratio of the nozzle that feeds the tube. The steepness of the curve at higher Mach numbers shows, however, that in this region large increases in Mach number result in only small increases in  $\lambda \frac{L}{D}$ . A Mach number of infinity at the entrance, which requires an infinite divergence ratio, gives a finite value of  $\lambda \frac{L}{D}$ ; namely, 0.206. If it is assumed from inspection of figure 15 that the mean value of  $\lambda$  is of the order of 0.0025, then the maximum possible value of  $\frac{L}{D}$  is 82.2. Only if  $\lambda$  approaches zero as the Mach



number approaches infinity, will it be possible to obtain infinite or even very large lengths in supersonic flow.

#### Flow with Shock

The region to the left of curve A may include a shock in the course of flow, provided the pressure in the exhaust space is great enough; on the other hand, the region between curves A and B must include a shock. Along curve B the Mach number, which is less than 1 following the shock, has attained 1 at the exit. Between curves A and B the Mach number is less than 1 at the exit and greater than 1 at the entrance. An interval of length corresponding to this interval may be subdivided into a supersonic interval corresponding to the region above curve A, a subsonic interval corresponding to the region below curve C, and an interval within which the shock occurs. The velocity distribution will not always be stable enough to make the curves of constant pressure ratio applicable.

The region between curves B and C is an imaginary region in which flow with a stable velocity distribution with or without a shock cannot exist.

#### REFERENCES

1. Grashof, F.: Theoretische Maschinenlehre. L. Voss (Leipzig), 1875, pp. 593-597.
2. Zeuner, G.: Technical Thermodynamics. (Leipzig), 1900, pp. 264-273.
3. Stodola, A.: Steam and Gas Turbines. Vol. I. McGraw-Hill Book Co., Inc., 1927, p. 61.
4. Frössel, W.: Flow in Smooth Straight Pipes at Velocities above and below Sound Velocity. NACA TM No. 844, 1938.
5. Keenan, Joseph H.: Friction Coefficients for the Compressible Flow of Steam. Jour. Appl. Mech. (Trans. A.S.M.E.), vol. 6, no. 1, March 1939, pp. A-11 - A-20.

6. Mueller, C., and O'Connell, R.: Friction Factors for Air Flowing in Straight Pipes at Supersonic Velocities. B. S. Thesis, Mech. Eng. Dept., M.I.T., 1941.
7. Instruments and Apparatus Special Subcommittee on the Measurement of Fluid Flow: Flow Measurement, 1940. Information on Instruments and Apparatus. Pt. 5. Measurement of Quantity of Materials. Ch. 4. Flow Measurement by Means of Standardized Nozzles and Orifice Plates. A.S.M.E. Power Test Codes. New York, N. Y. 1940.
8. Huron, F., and Nelson, N.: Investigation of Supersonic Flow in Nozzles and Tubes. M. S. Thesis, Naval Arch. Dept., M.I.T., 1944.
9. Shapiro, Ascher H.: Nozzles for Supersonic Flow without Shock Fronts. (Paper presented at the Annual Meeting of the A.S.M.E., New York, N. Y., Nov. 29 to Dec. 3, 1943.) Jour. Appl. Mech. (Trans. A.S.M.E.), vol. 11, no. 2, June 1944, pp. A-93 - A-100.
10. Meyer, Th.: Über zweidimensionale Bewegungsvorgänge in einem Gas, das mit Überschallgeschwindigkeit strömt. Mitteilungen über Forschungsarbeiten auf dem Gebiete des Ing.-Wes., vol. 62, 1908, pp. 31-67.
11. Kirsten, H.: Experimentelle Untersuchung der Entwicklung der Geschwindigkeitsverteilung bei der turbulenten Rohrströmung. Diss. (Leipzig), 1927.
12. Brooks, Craft, and Montrello: Friction Factor for Turbulent Flow in Transition Region for Straight Pipe. M. S. Thesis, Naval Arch. Dept., M.I.T., 1943.
13. Hawthorne, W. R.: Simplified Analysis of Frictional and Compressible Flow in Pipes. RAE, S. Farnborough. Note No. E. 3929, March 1942.
14. Young, A. D., and Winterbottom, N. E.: High Speed Flow in Smooth Cylindrical Pipes of Circular Section. RAE, S. Farnborough. Rep. No. Aero. 1785, Nov. 1942.

TABLE I

TEST 1

Nozzle A; nozzle throat diam., 0.375 in.; tube diam., 0.375 in.; inlet temperature, 126° F; inlet pressure, 16,179 lb/sq ft abs.; tube length, 10 ft; flow per unit area, 188.2 lb/sec sq ft

x (ft)	p (lb/sq ft abs.)	$\bar{\lambda}$ (a)	M	Re (b)	T (°F abs.)	V (fps)
-----	<sup>c</sup> 4,527.3	-----	-----	-----	-----	-----
10	4,288	-----	<sup>c</sup> 1.00	<sup>c</sup> 5.14x10 <sup>5</sup>	<sup>c</sup> 488.3	<sup>c</sup> 1085.4
9.75	5,652	0.00313	.824	4.91	516	917.0
9	7,448	.00326	.640	4.74	541	730.4
8	8,879	.00322	.543	4.75	553	625.9
7	9,956	.00323	.485	4.62	560	564.4
6	10,866	.00327	.447	4.58	563	520.8
5	11,682	.00327	.417	4.57	565	486.9
4	12,420	.00328	.392	4.55	569	459.7
3	13,102	.00333	.372	4.54	570	437.2
2	13,751	.00321	.356	4.54	571	417.4
1	14,336	.00386	.342	4.53	572	401.2
0	15,004	-----	.326	4.52	574	384.1

<sup>a</sup>Average  $\lambda$ , from x = 1 ft to x = 9.75 ft = 0.003224.

<sup>b</sup>Average Re from x = 1 ft to x = 9.75 ft = 4.63 x 10<sup>5</sup>.

<sup>c</sup>From calculated pressure at state of maximum entropy.

TABLE II

TEST 2

Nozzle A; nozzle throat diam., 0.375 in.; tube diam., 0.375 in.; inlet temperature, 125° F; inlet pressure, 17,607 lb/sq ft abs.; tube length, 10 ft; flow per unit area, 188.0 lb/sec sq ft

x (ft)	p (lb/sq ft abs.)	$\bar{\lambda}$ (a)	M	Re (b)	T (°F abs.)	V (fps)
10	-----	-----	-----	-----	-----	-----
9.75	10,355	0.00318	0.466	4.61x10 <sup>5</sup>	560	543.1
9	10,998	.00326	.440	4.61	562	513.6
8	11,789	.00314	.414	4.61	564	481.8
7	12,491	.00316	.390	4.56	566	455.8
6	13,143	.00322	.370	4.56	567	433.8
5	13,764	.00326	.354	4.56	568	414.9
4	14,352	.00328	.341	4.54	571	399.0
3	14,917	.00326	.328	4.54	572	384.6
2	15,452	.00325	.317	4.54	572 <sup>+</sup>	371.7
1	15,964	.00386	.307	4.52	573	360.3
0	16,546	-----	.296	4.52	574	348.1

<sup>a</sup>Average  $\lambda$ , from x = 1 ft to x = 9.75 ft = 0.00322.

<sup>b</sup>Average Re from x = 1 ft to x = 9.75 ft = 4.55 x 10<sup>5</sup>.

TABLE III  
TEST 3

Nozzle A; nozzle throat diam., 0.375 in.; tube diam., 0.375 in.; inlet temperature, 126° F; inlet pressure, 7,422.1 lb/sq ft abs.; tube length, 10 ft; flow per unit area, 82.77 lb/sec sq ft

x (ft)	p (lb/sq ft abs.)	$\bar{\lambda}$ (a)	M	Re (b)	T (°F abs.)	V (fps)
10	2008.1	-----	-----	-----	431	1057.1
9.75	2561.3	0.00386	0.790	2.19x10 <sup>5</sup>	506	873.5
9	3391.1	.00386	.790	2.11	530	690.6
8	4052.2	.00384	.790	2.11	542	589.8
7	4558.4	.00380	.790	2.11	547	529.7
6	4987.1	.00385	.790	2.11	550	487.4
5	5368.4	.00387	.393	2.05	552	454.8
4	5717.3	.00389	.393	2.05	554	428.5
3	6040.9	.00392	.393	2.05	555	406.8
2	6342.4	.00385	.393	2.05	557	388.3
1	6624.6	.00448	.393	2.03	559	372.4
0	6934.3	-----	.307	2.03	559.4	356.4

<sup>a</sup>Average  $\lambda$ , from x = 1 ft to x = 9.75 ft = 0.00386.

<sup>b</sup>Average Re from x = 1 ft to x = 9.75 ft = 2.069 x 10<sup>5</sup>.

TABLE IV  
TEST 4

Nozzle A; nozzle throat diam., 0.375 in.; tube diam., 0.375 in.; inlet temperature, 126° F; inlet pressure, 4,146.5 lb/sq ft abs.; tube length, 10 ft; flow per unit area, 42.01 lb/sec sq ft

x (ft)	p (lb/sq ft abs.)	$\bar{\lambda}$ (a)	M	Re (b)	T (°F abs.)	V (fps)
10	-----	-----	-----	-----	---	-----
9.75	2150.3	-----	0.485	1.082x10 <sup>5</sup>	523	545.4
9	2357.3	0.00456	.485	1.082	523	501.2
8	2595.5	.00455	.485	1.082	523	458.2
7	2807.4	.00459	.485	1.082	523	425.4
6	2999.3	.00459	.485	1.082	523	399.7
5	3176.3	.00459	.333	1.067	536	378.2
4	3341.2	.00459	.333	1.067	536	360.6
3	3493.7	.00449	.333	1.067	536	345.3
2	3640.0	.00459	.333	1.067	536	331.9
1	3778.2	.00451	.333	1.067	536	320.2
0	3930.1	.00515	.269	1.061	540	308.0

<sup>a</sup>Average  $\lambda$ , from x = 1 ft to x = 9.75 ft = 0.00456.

<sup>b</sup>Average Re from x = 1 ft to x = 9.75 ft = 1.075 x 10<sup>5</sup>.

TABLE V

TEST 10

Nozzle throat diam., 0.562 in.; tube diam., 0.945 in.

Date: 4-23

Inlet temperature 143 F; inlet pressure 85.5 lb/sq in abs.;  
flow per unit area in tube, 93.46 lb/sec sq ft.

$\frac{L}{D}$	$\frac{P}{P_1}$	$\bar{\lambda}$	$Re \times 10^{-5}$	M
0-	0.0747			
0+	.0721			2.06
1.59	.0777	0.00482	8.74	1.96
3.18	.0800	.00189	8.58	1.92
4.76	.0806	.00053	8.51	1.91
7.94	.0843	.00150	8.41	1.85
9.52	.0877	.00265	8.24	1.80
12.69	.0971	.00342	7.98	1.67
15.87	.1044	.00250	7.65	1.58
17.55	.1071	.00161	7.50	1.55
19.04	.1112	.00264	7.39	1.51
20.69	.1151	.00257	7.29	1.47
22.21	.1203	.00293	7.18	1.42
25.38	.1293	.00222	7.10	1.34

Date: 4-29

Inlet temperature 147 F; inlet pressure 84.7 lb/sq in abs.;  
flow per unit area in tube 92.24 lb/sec sq ft.

0-	0.0744			
0+	.0730			2.06
1.59	.0780	0.00426	8.61	1.96
3.18	.0801	.00174	8.40	1.93
4.76	.0817	.00130	8.30	1.90
6.35	.0842	.00206	8.22	1.86
7.94	.0849	.00057	8.11	1.84
9.52	.0882	.00256	8.02	1.82
12.69	.0986	.00378	7.79	1.65
15.87	.1055	.00229	7.47	1.57
17.55	.1088	.00195	7.30	1.54
19.04	.1116	.00181	7.22	1.52
20.69	.1164	.00261	7.13	1.46
22.21	.1206	.00235	7.02	1.42
23.89	.1259	.00250	6.90	1.37
25.38	.1299	.00204	6.81	1.34

TABLE VI

TEST 11

Nozzle throat diam., 0.186 in.; tube diam., 0.498 in.

Date: 12-8

Inlet temperature, 88 F; inlet pressure, 189.0 lb/sq in abs.;  
flow per unit area in tube, 85.47 lb/sec sq ft.

$\frac{L}{D}$	$\frac{P}{P_1}$	$\bar{\lambda}$	$Re \times 10^{-5}$	M
1.39	0.0161		6.96	2.98
3.77	.0178	0.00307	6.46	2.80
5.77	.0179	.00024	6.40	2.79
7.78	.0187	.00151	6.10	2.72
9.79	.0197	.00212	5.92	2.63
11.80	.0217	.00397	5.63	2.48
15.81	.0241	.00231	5.22	2.31
19.83	.0262	.00194	4.98	2.19
23.85	.0301	.00347	4.61	1.99
27.86	.0314	.00111	4.48	1.93
31.88	.0356	.00340	4.27	1.76
35.89	.0404	.00343	3.97	1.61
37.90	.0420	.00190	3.92	1.56

Date: 12-15

Inlet temperature, 97 F; inlet pressure 190.2 lb/sq in abs.;  
flow per unit area in tube, 85.33 lb/sec sq ft.

.13	0.0148		7.34	3.14
1.39	.0160	0.00440	6.86	3.00
3.77	.0179	.00343	6.14	2.78
5.77	.0181	.00033	6.13	2.77
9.79	.0199	.00174	5.88	2.62
11.80	.0219	.00416	5.45	2.46
15.81	.0241	.00214	5.16	2.31
19.83	.0258	.00159	4.94	2.21
23.85	.0304	.00417	4.47	1.97
27.86	.0332	.00226	4.28	1.85
31.88	.0347	.00117	4.08	1.80
35.89	.0391	.00328	3.96	1.65
37.90	.0411	.00265	3.88	1.59

TABLE VII

## TEST 12

Nozzle throat diam., 0.175 in.; tube diam., 0.4375 in.;  
inlet temperature, 87 F; inlet pressure 194.3 lb/sq in abs.;  
flow per unit area in tube, 100.9 lb/sec sq ft.

$\frac{L}{D}$	$\frac{P}{P_1}$	$\bar{\lambda}$	$Re \times 10^{-5}$	M
.57	0.0191		7.03	2.91
4.05	.0239	0.00391	5.94	2.54
6.07	.0250	.00171	5.81	2.45
8.10	.0268	.00266	5.74	2.36
10.12	.0275	.00103	5.46	2.32
12.14	.0278	.00046	5.40	2.29
14.17	.0296	.00267	5.17	2.20
20.43	.0358	.00275	4.66	1.96
24.29	.0401	.00265	4.52	1.78
28.34	.0449	.00268	4.16	1.65
32.39	.0498	.00245	4.00	1.53
36.44	.0571	.00288	3.80	1.38

TABLE IX

## TEST 14

Nozzle throat diam., 0.186 in.; tube diam., 0.498 in.;  
inlet temperature, 76.5 F; inlet pressure, 2108.0 lb/sq ft abs.;  
flow per unit area in tube, 6.64 lb/sec sq ft.

$\frac{L}{D}$	$\frac{P}{P_1}$	$\bar{\lambda}$	$Re \times 10^{-5}$	M
.13	0.0174		0.519	2.84
1.39	.0189	0.00510	.484	2.69
3.77	.0208	.00340	.442	2.52
5.77	.0211	.00043	.441	2.51
7.78	.0226	.00313	.430	2.40
9.79	.0229	.00047	.427	2.38
11.8	.0235	.00121	.419	2.34
15.8	.0245	.00098	.406	2.28
19.8	.0259	.00129	.394	2.19
23.9	.0293	.00307	.367	2.01
27.9	.0343	.00416	.336	1.80
31.9	.0414	.00506	.309	1.57
35.9	.0508	.00516	.286	1.34
37.9	.0582	.00555	.273	1.20

TABLE VIII

## TEST 13

Nozzle throat diam., 0.107 in.; tube diam., 0.498 in.

Date: 8-7

Inlet temperature, 88.5 F; inlet pressure, 201.2 lb/sq in abs.;  
flow per unit area in tube, 30.1 lb/sec sq ft.

$\frac{L}{D}$	$\frac{P}{P_1}$	$\bar{\lambda}$	$Re \times 10^{-5}$	M
1.39	0.00378			3.64
3.77	.00421	0.00244	3.12	3.42
5.77	.00458	.00254	2.84	3.29
7.78	.00490	.00209	2.70	3.13
9.79	.00499	.00063	2.69	3.10
11.8	.00548	.00315	2.47	2.94
15.8	.00638	.00289	2.26	2.66
19.8	.00728	.00274	2.02	2.44
23.9	.00815	.00256	1.87	2.26
27.9	.00914	.00274	1.75	2.10
31.9	.01013	.00265	1.64	1.96
35.9	.01135	.00298	1.60	1.81
39.9	.01307	.00378	1.47	1.63
43.9	.01495	.00387	1.37	1.46
47.9	.01745	.00342	1.30	1.31
50.0	.01939	.00419	1.24	1.20

Date: 9-2

Inlet temperature, 86 F; inlet pressure, 200.7 lb/sq in abs.;  
flow per unit area in tube, 30.1 lb/sec sq ft.

.13	0.00344		3.65	3.87
1.39	.00374	0.00334	3.38	3.70
3.77	.00422	.00295	3.62	3.45
5.77	.00435	.00203	2.73	3.19
9.79	.00490	.00058	2.68	3.15
11.8	.00534	.00293	2.49	3.04
15.8	.00620	.00274	2.23	2.72
19.8	.00728	.00331	2.00	2.46
23.9	.00803	.00220	1.87	2.31
27.9	.00907	.00294	1.70	2.12
35.9	.01104	.00253	1.56	1.86
39.9	.01274	.00384	1.46	1.67
43.9	.01457	.00355	1.38	1.52
47.9	.01729	.00420	1.30	1.33
50.0	.01926	.00435	1.24	1.21

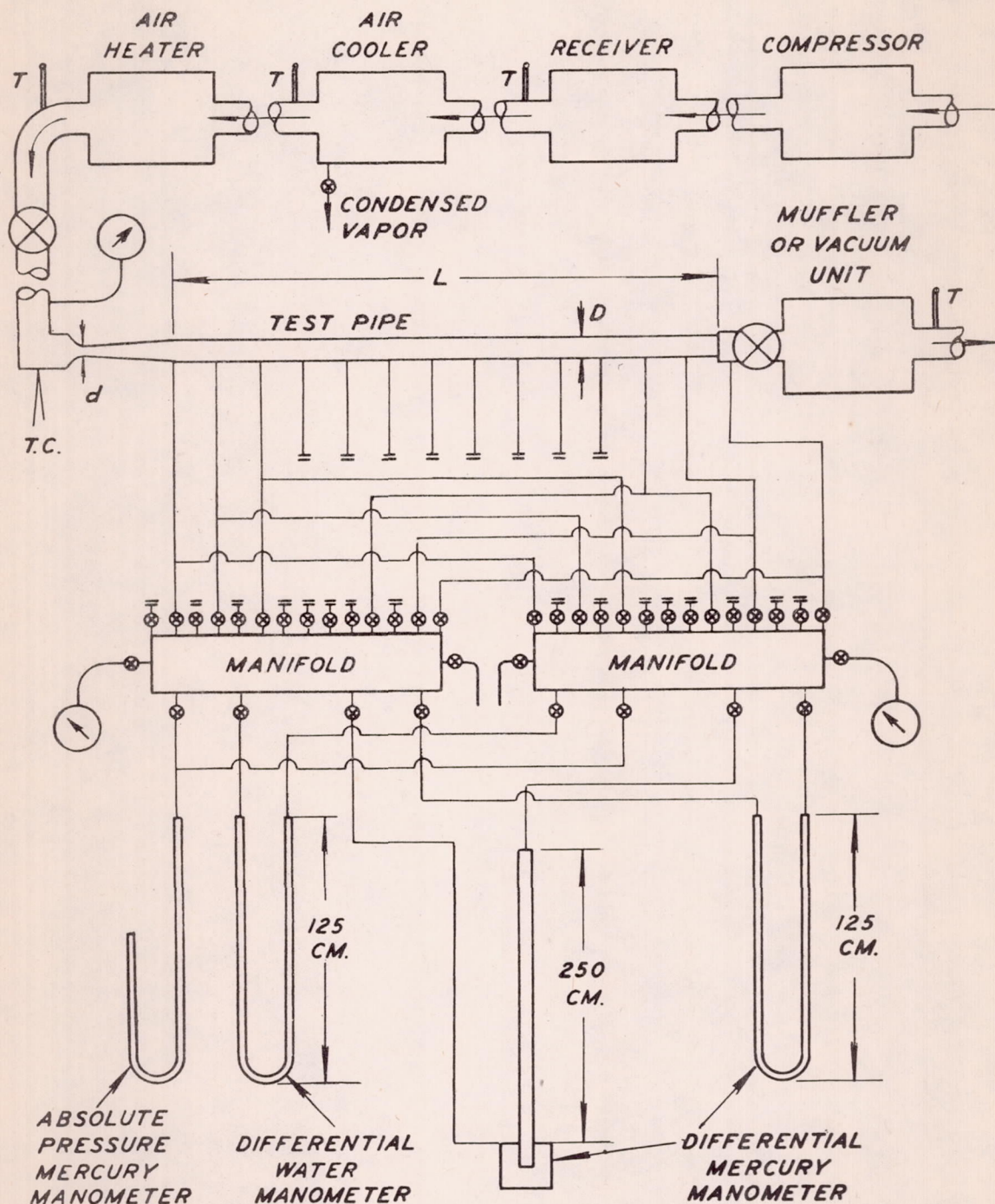


Figure 1.- Schematic diagram of test apparatus.

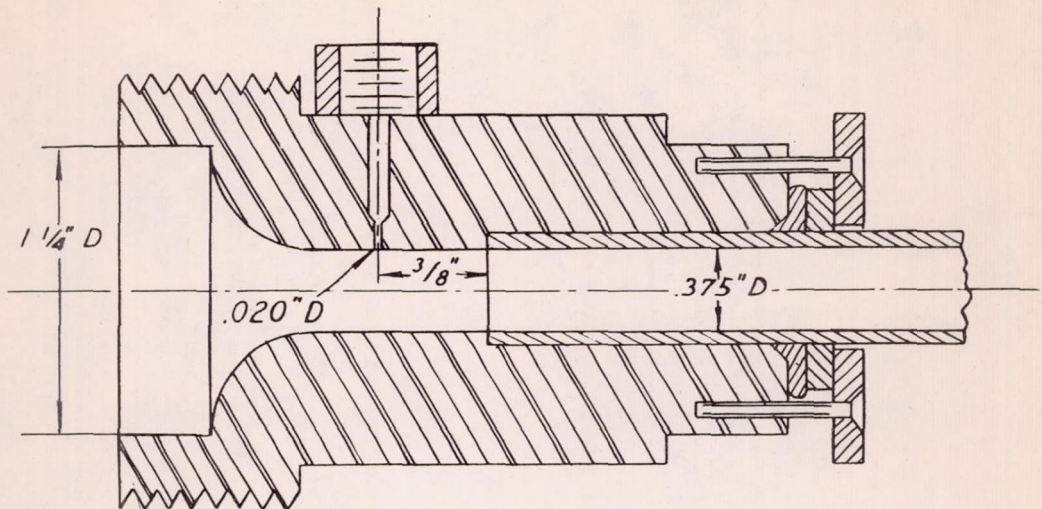


Figure 2.- Entrance nozzle A.

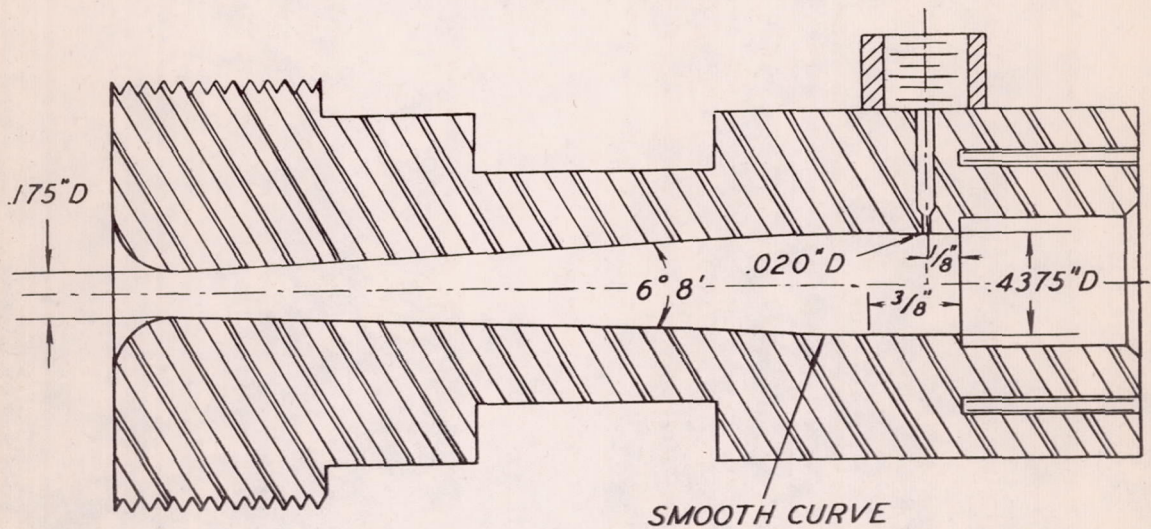
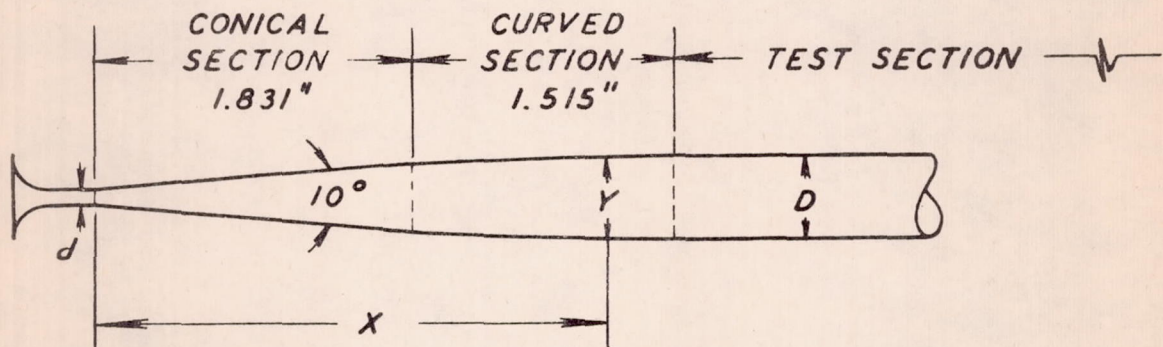
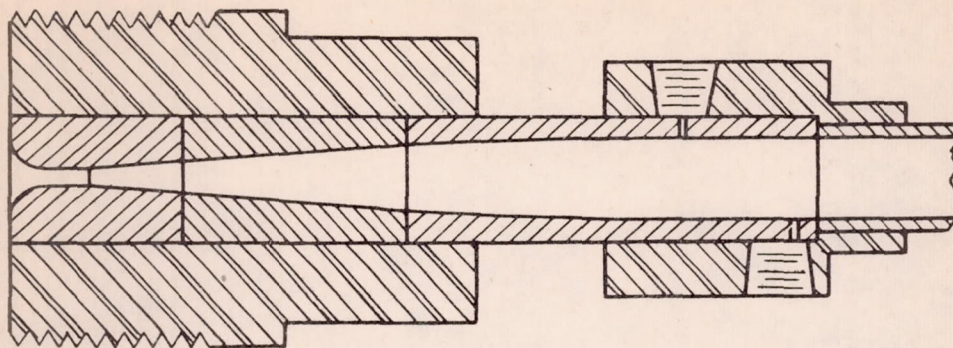


Figure 3.- Entrance nozzle B.





Dimensions for nozzle contour  
 $d = 0.107$ -in.-diam.     $D = 0.495$ -in.-diam.

x	Y
inches	inches
0	0.107
1.831	0.427
1.855	0.431
1.887	0.436
1.914	0.440
1.943	0.444
1.977	0.448
2.022	0.453
2.062	0.457
2.107	0.461
2.158	0.465
2.231	0.470
2.301	0.474
2.379	0.478
2.511	0.483
2.661	0.487
2.876	0.491
3.036	0.493
3.143	0.494
3.346	0.495

Entrance nozzle D is entrance nozzle C with the throat bored out to a diameter of 0.186 inch.

Figure 4. - Entrance nozzle C.

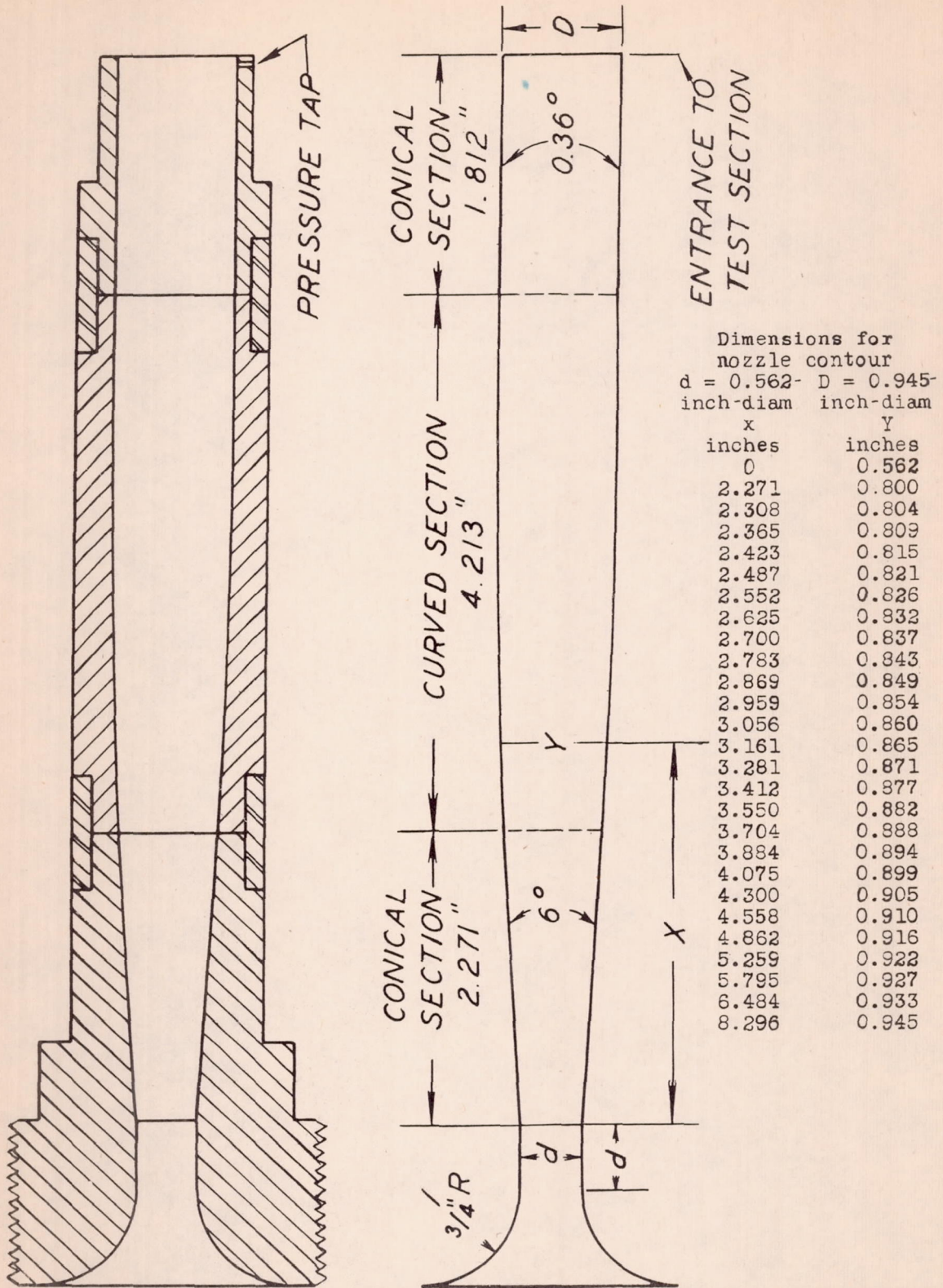


Figure 5.- Entrance nozzle E.

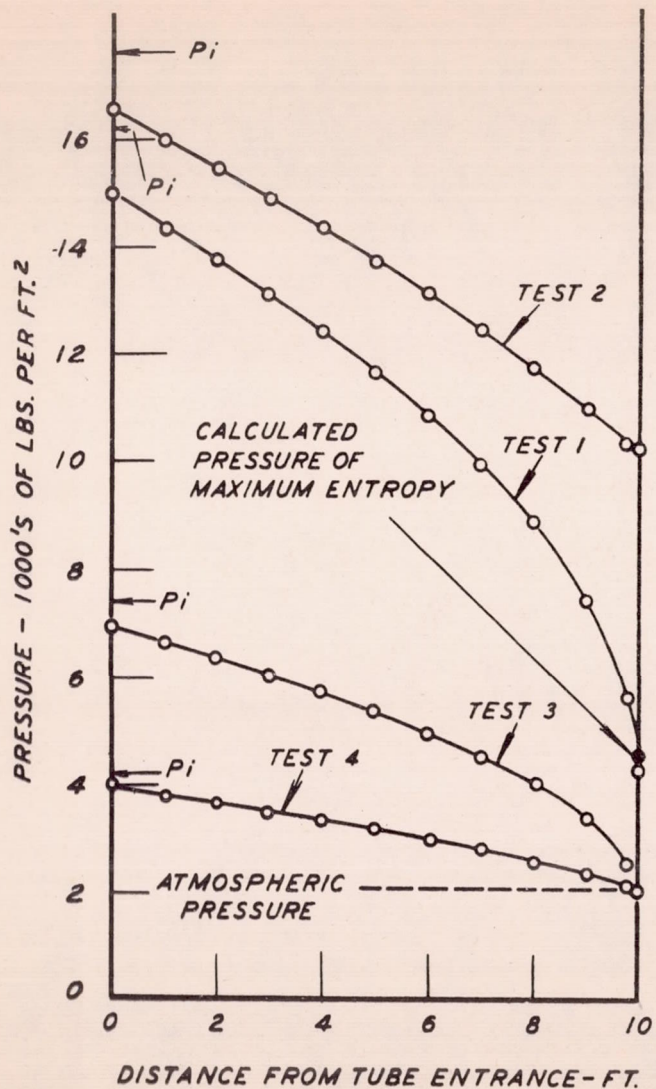


Figure 6.- Pressure distribution along the test pipe for subsonic flow.

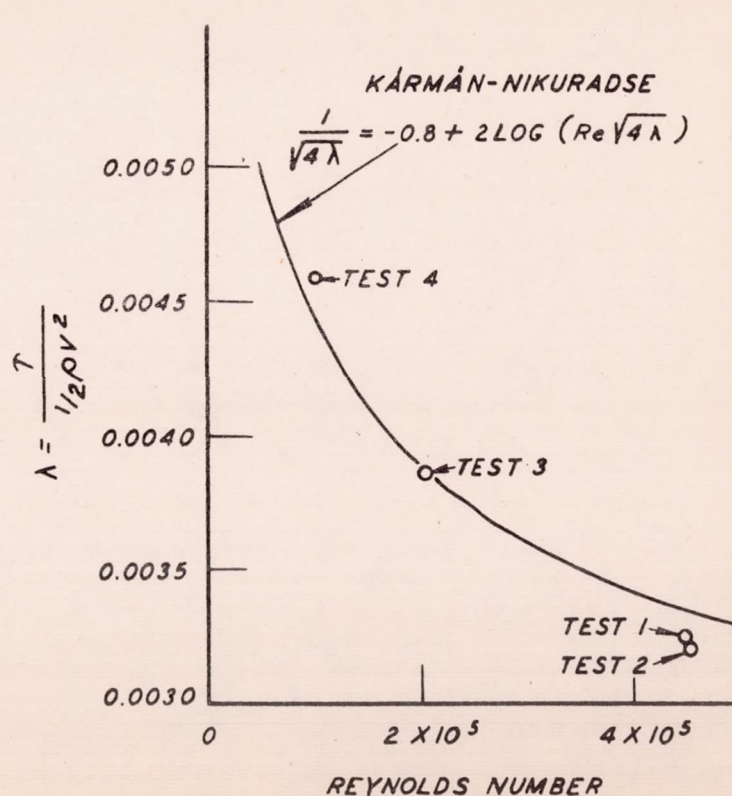


Figure 7.- Friction coefficients for subsonic flow compared with those for incompressible flow.

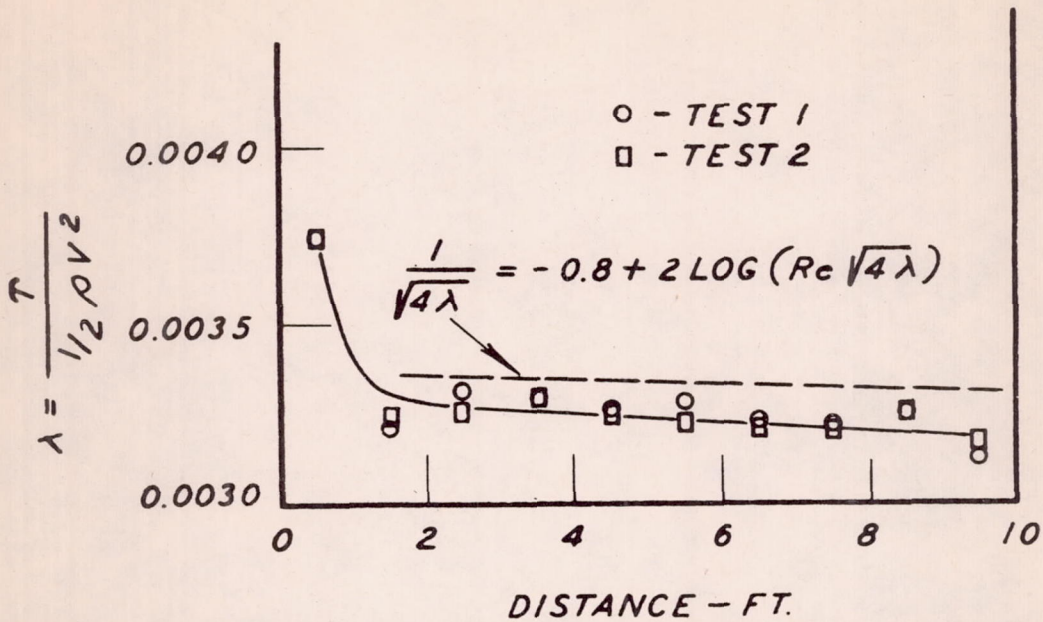


Figure 8.- Friction coefficient against distance along pipe for subsonic flow.

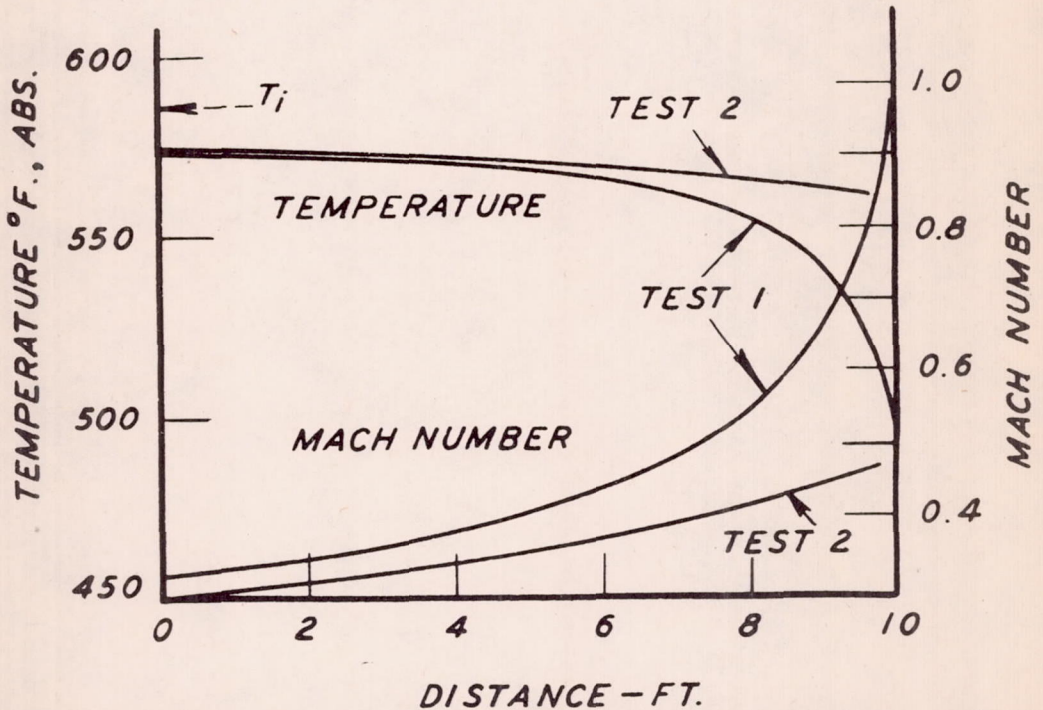


Figure 9.- Temperature and Mach number against distance along pipe for subsonic flow.

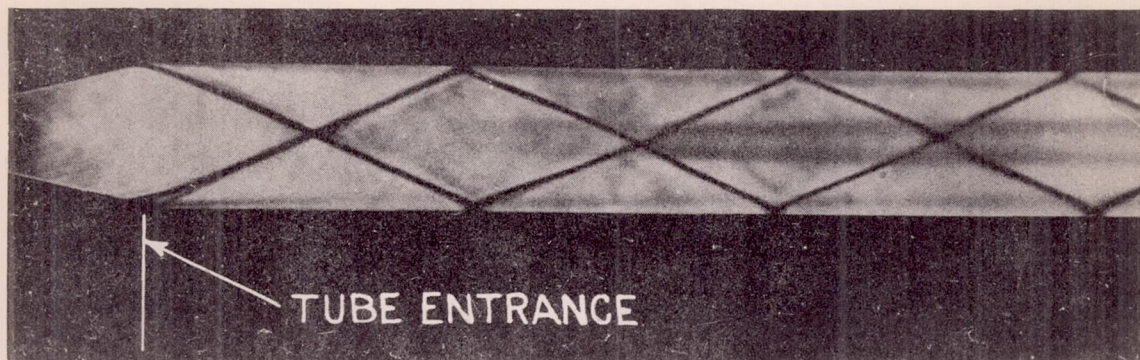


Figure 10.- Schlieren photograph of oblique shock fronts formed at the entrance to a tube of rectangular cross-section. Divergence ratio = 3.50,  $\theta = 30^\circ$ , depth of passage perpendicular to the plane of photograph = 0.400", cross-sectional area of parallel passage = 0.280 square in. Exposure time 1/10 second (photograph from reference 8).

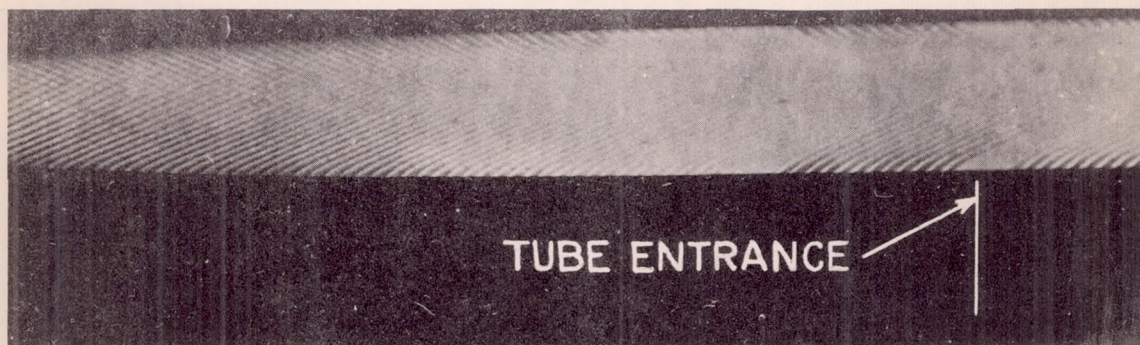


Figure 11.- Schlieren photograph of nozzle with the transition length from the diverging passage to the parallel passage designed to avoid oblique shock fronts. Divergence ratio = 3.50, depth of passage perpendicular to the plane of photograph = 0.400", cross-sectional area of parallel passage = 0.280 square in. Exposure time 1/10 second (photograph from reference 8).

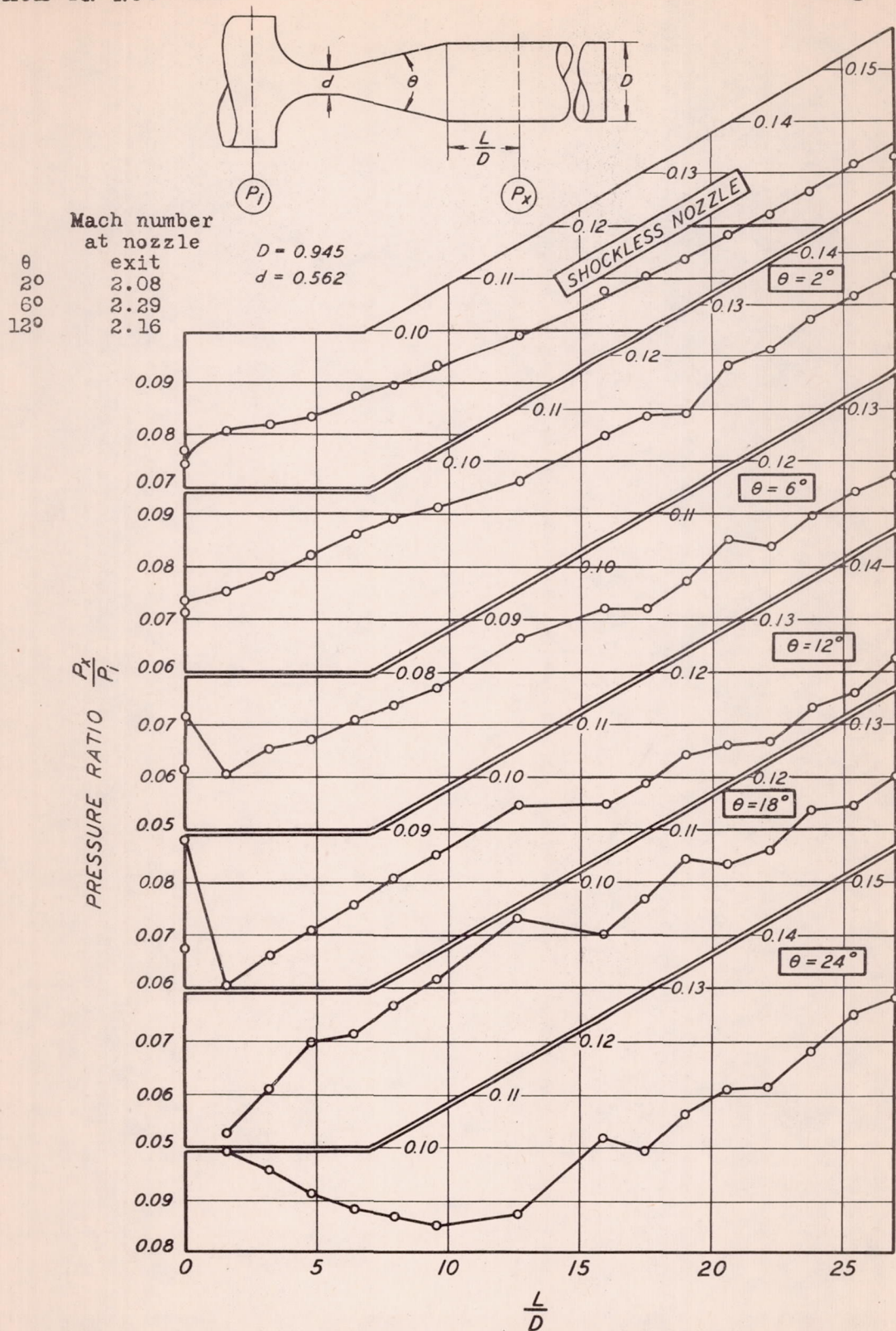


Figure 12. Pressure ratio against distance along pipe using entrance nozzles with different angles of divergence ( $\theta$ ).

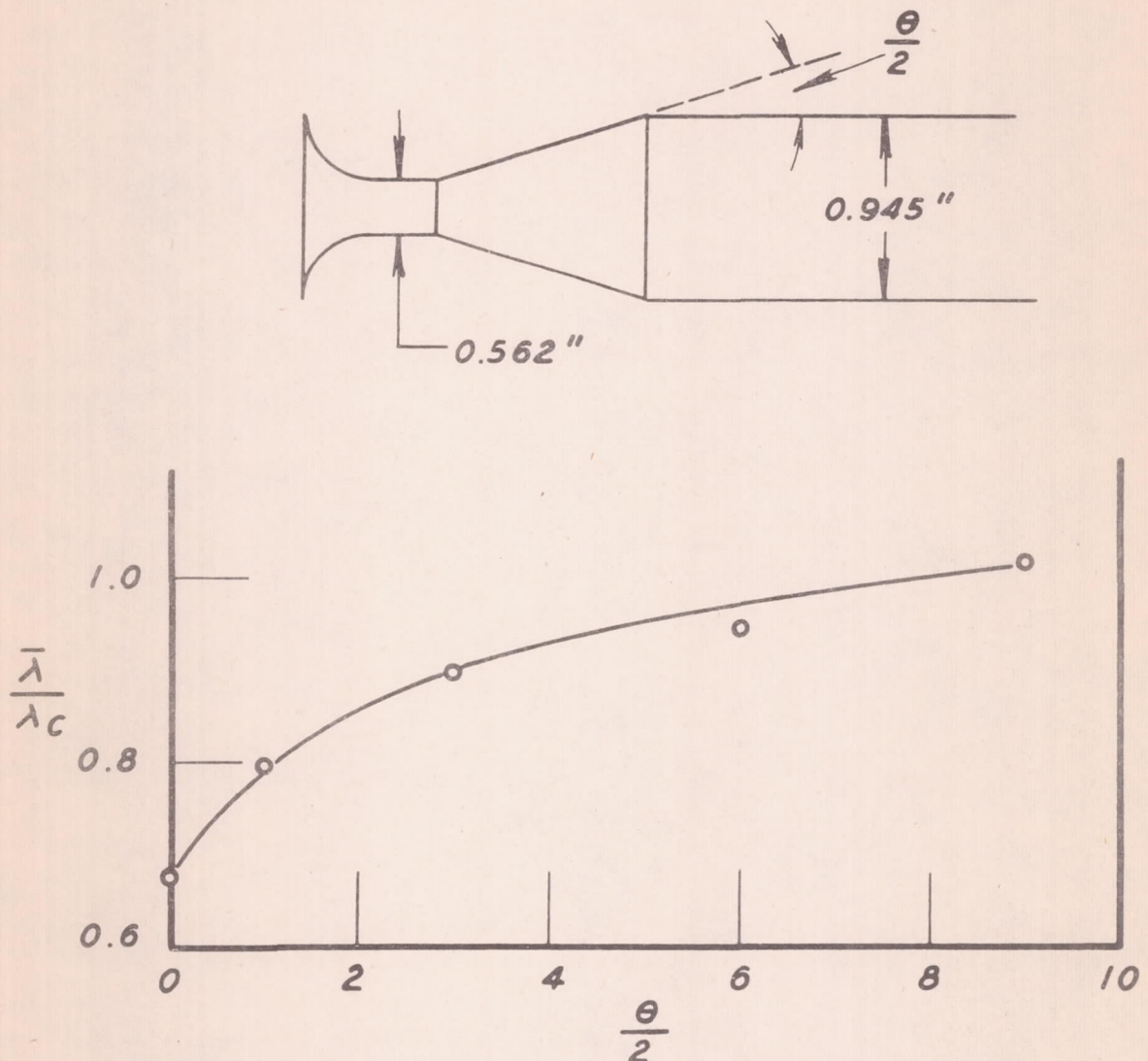


Figure 13.- Ratio of the measured apparent friction coefficient ( $\bar{\lambda}$ ) to the friction coefficient for incompressible flow ( $\lambda_c$ ) against angle of divergence ( $\theta$ ). The friction coefficient is the mean value of the apparent friction coefficient for the interval of test section from  $L/D = 1.59$  to  $L/D = 26.98$ . The value of  $\lambda_c$  was computed from the von Karman-Nikuradse relation between Reynolds number and friction coefficient.

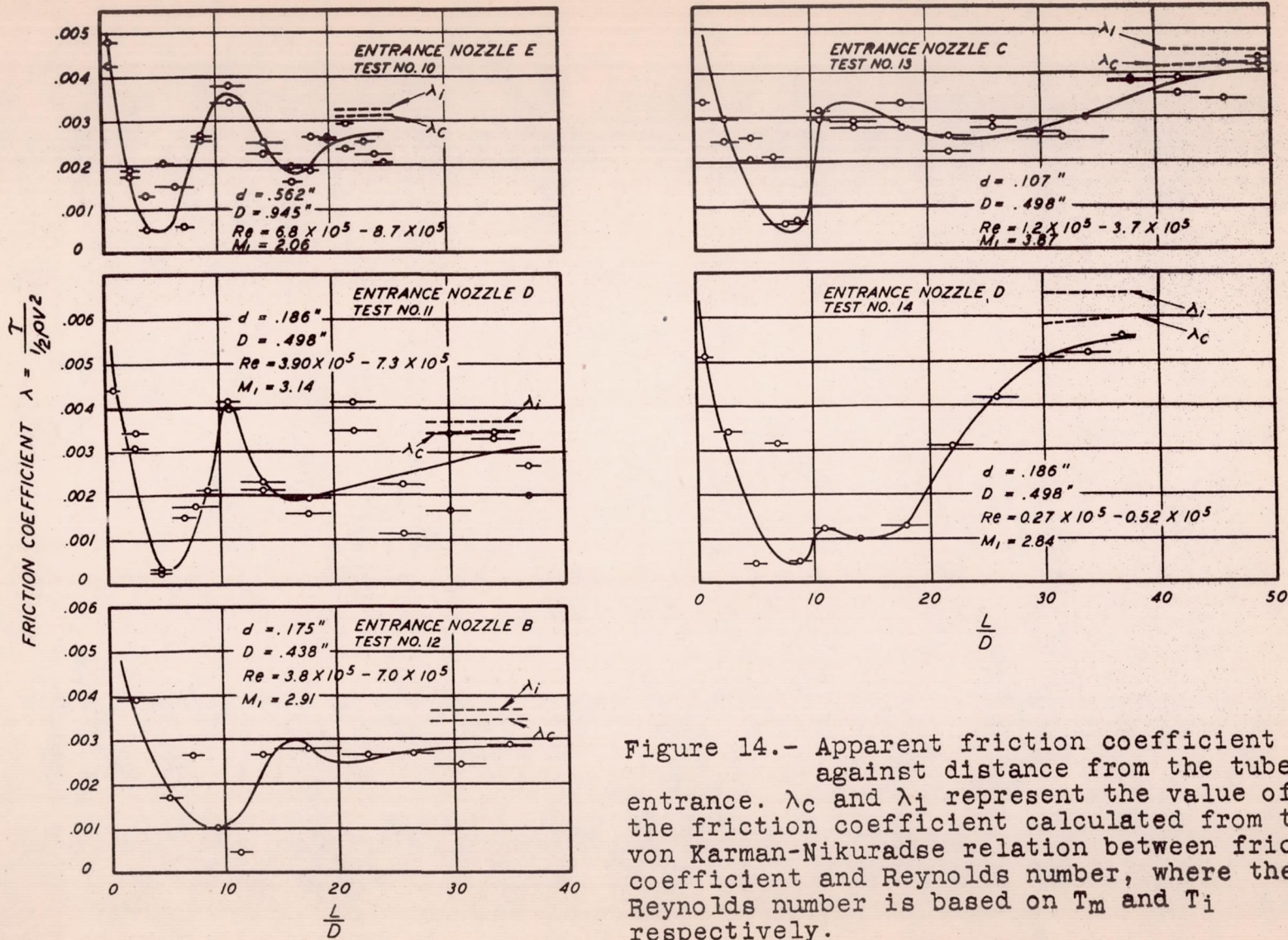


Figure 14.- Apparent friction coefficient against distance from the tube entrance.  $\lambda_c$  and  $\lambda_i$  represent the value of the friction coefficient calculated from the von Karman-Nikuradse relation between friction coefficient and Reynolds number, where the Reynolds number is based on  $T_m$  and  $T_i$  respectively.



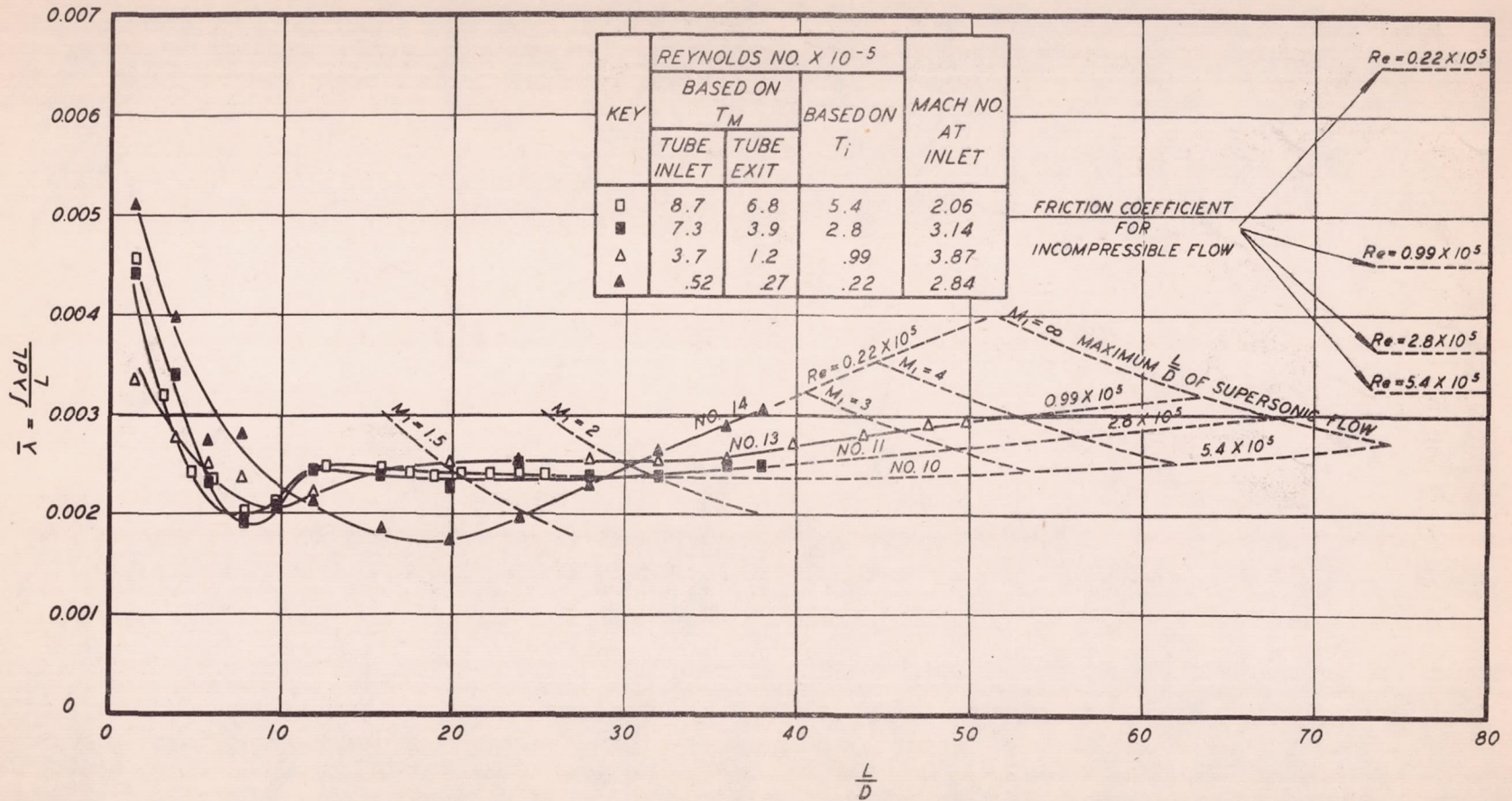


Figure 15.- Mean apparent friction coefficient against L/D.

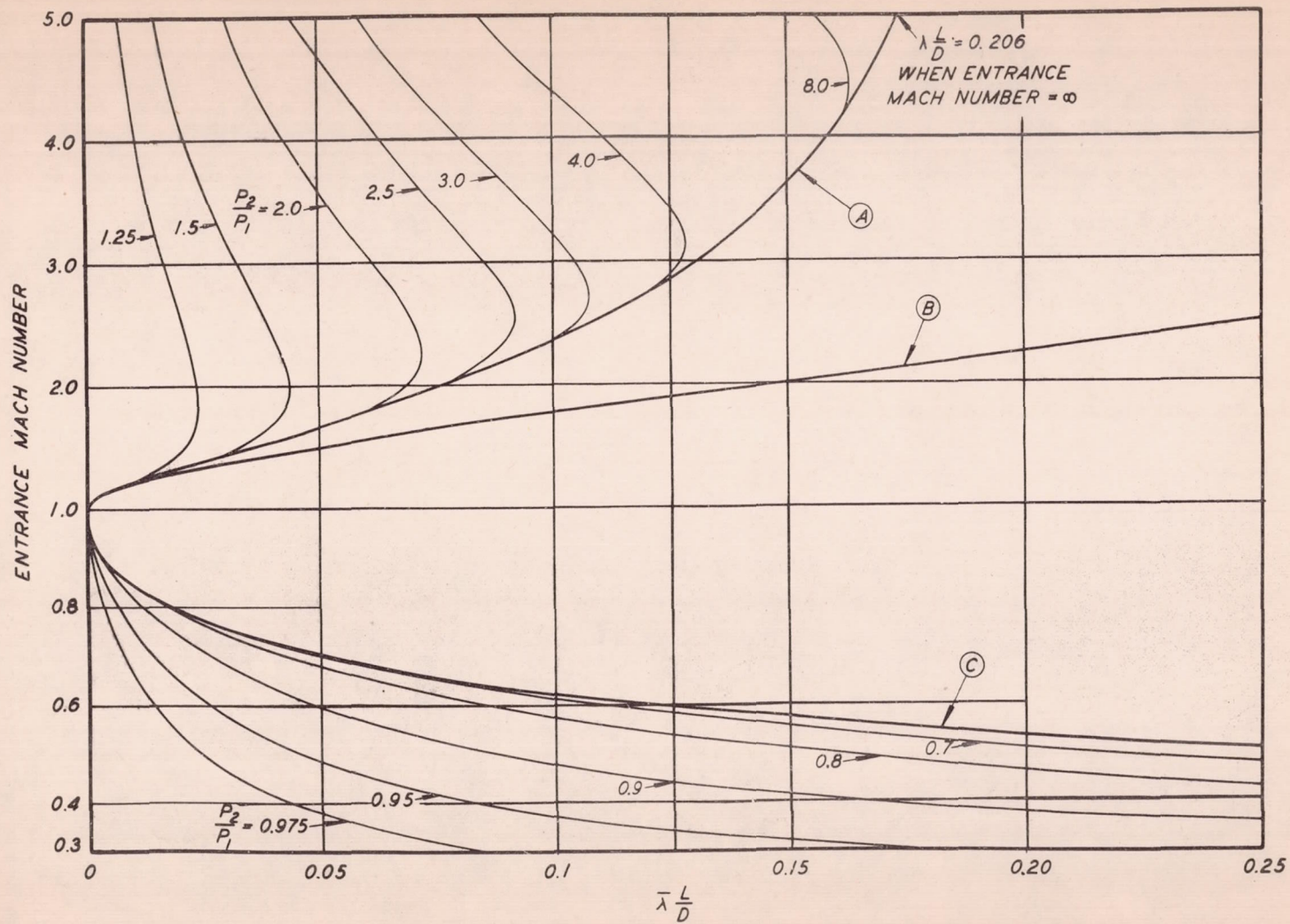


Figure 16. - Entrance Mach number against  $\lambda \frac{L}{D}$ .  $P_1$  and  $P_2$  represent the pressure at the entrance and exit, respectively, of the constant area section.